



DESY Summer student programme 2014
Hamburg, July 22 – September 11

**Development of software for design, optimization and operation of
X-ray compound refractive lens systems**

Roman Kirtaev
Moscow Institute of Physics and Technology

Supervised by Dmitri Novikov
DESY Photon Science

Contents

1 Introduction and motivation	3
1.1 Construction of new beamlines of PETRA extension	3
1.2 Russian-German nanodiffraction beamline (P23) at PETRA extension	4
1.3 Beamline layout.....	6
2 Beamline optics	7
2.1 Necessary requirements to the beamline optics.....	7
2.2 Beamline optics layout. Source properties	7
3 Focusing with lenses	10
3.1 Basic facts: geometrical optics	10
3.2 Coherent X-ray focusing. Ray transfer matrix analysis	12
4 Software implementation	15
4.1 General calculation flow, optics optimization and geometry	15
4.2 Transmission and beam loss factor.....	17
4.3 Output.....	17
5 Application examples	19
5.1 Single transfocator.....	19
5.2 Two transfocators (parallel beam).....	20
5.3 Two transfocators (“aperture matching”).....	21
5.4 Selection of beam size calculation method	23
Conclusion.....	24
Acknowledgement.....	24
References	24

1 Introduction and motivation

The main aim of my work was to create a software package that can be used for designing a configuration of CRL-based (compound refractive lens) optics in accordance with:

- type of the experiment (make divergent/convergent/parallel beam)
- minimization of total amount and types of lenses
- maximization of photon flux after the optical system

The optimized design of the CRL optics should be capable of covering the working X-ray energy range from 15keV to 35 keV

1.1 Construction of new beamlines of PETRA extension

The PETRA III extension project adds two new experimental halls on either side (North and East) of the existing “Max-von-Laue Hall” facilities making use of the long straight section and part of the adjacent arcs (Fig. 1.1.1).



Figure 1.1.1. View of the PETRA III storage ring (red line). The present experimental hall is shown together with the planned additional experimental halls in the North and East.

The northern straight section already accommodates one of two 40 m long damping wiggler arrays producing an extremely hard and powerful X-ray beam which will also be utilized for materials science experiments. The long straight section in the west is available for additional insertion devices. In order to accommodate insertion device sources in the arc sections, which were filled with long dipole magnets yielding a rather soft X-ray spectrum, the machine lattice will be modified. The new lattice adds double bent achromat (DBA) cells in the arcs, each allowing for a 5 m long straight section. Similar to the present PETRA III beamlines, these straights will serve two beamlines

independently by use of canting dipoles resulting in two separate 2 m long straights. Different from the present 5 mrad canting scheme, a canting angle of 20 mrad was chosen at the extension beamlines to provide more spatial flexibility for the experiments further downstream. In total, the new lattice provides eight short straight high- β sections in the two arcs making them very suitable for the use of undulators. Overall, 11 new beamlines will be built in different phases. Five of the new beamlines will be designed as "short undulator" beamlines continuing most of the productive techniques formerly provided at DORIS III bending magnet beamlines. These sources will not only be very well suited for the spectrum of applications to be relocated from DORIS III but also provide a considerably brighter beam. In addition, four high-brilliance long undulator beamlines will be built in PETRA III hall East, three of them in collaboration with international partners, Sweden, India and Russia.

1.2 Russian-German nanodiffraction beamline (P23) at PETRA extension

The main focus of the beamline will be on the application of in situ and in operando diffraction techniques for the study of low-dimensional and nanoscale systems, i.e. structural properties and especially their evolution during chemical processes or under non-ambient conditions, such as high pressure, low temperature, electrical and magnetic fields, laser irradiation etc.

Examples of scientific cases are:

Space averaging methods

The most common and demanded application of X-ray diffraction is conventional space averaging scattering from bulk and surface objects. One major focus lies on the investigation of catalytic processes and relevant materials. Conventional averaging X-ray diffraction techniques are e.g. being used for the investigation of atomic structure of surfaces. A large part of the in situ research is dedicated to liquid/solid interfaces, e.g. the growth of complex functional nanomaterials and their properties. Progress has especially been achieved in time-resolved investigations of phase transformations, such as crystallization of immobilized nanoparticles from the amorphous phase, electric field induced phase transitions and ferroelectric switching mechanisms.

Diffraction microscopy of bulk objects

Diffraction using X-ray microbeams has considerably widened the research possibilities at the nanoscale. This applies not only to novel nanoscaled objects, but also to investigations of already well-studied materials that can be re-visited with access to ultra-short length scales. The basic diffraction tomography analysis can be combined with X-ray fluorescence spectroscopy and XANES. Along with the phase analysis in complex polycrystalline structures, pencil beams are also used for the investigation of local strain tensors, stress and microstructure evolution in nanocrystalline materials. This technique is applicable to single crystals, composite and functional graded materials.

Diffraction microscopy of nanosized objects

Microbeam X-ray diffraction is gaining importance as an effective tool for studying single nanocrystalline objects and oriented arrays of such objects. Technically, the studies of individual objects at the nanoscale are very challenging and require, along with an extraordinary stability of the instrument and the X-ray optical system, a parallel application of state-of-the-art nano-sample handling and characterization techniques. Combination of microbeam diffraction with anomalous scattering to investigate distortions in scanning probe nanolithography demonstrated an opportunity to use nanoscale strain variations for the selection of the initial material state in ferroelectrics, dielectrics, and other complex oxides. Additional opportunities arise through the parallel use of atomic force microscopy which allows selective introduction of defects or simultaneous probing of elastic properties in single nanocrystals.

Coherent diffraction imaging of nanosized objects

Coherent Diffraction Imaging (CDI) can be applied to investigate two- and three-dimensional structures with a resolution at 10 nm scales. CDI has developed into a characterization method capable of observing also the inner structure of complex nanoparticles and measuring internal strain evolution in nanoparticles under extreme conditions.

X-ray Bragg diffraction ptychography

The advantages of CDI can be combined with the structural sensitivity of conventional X-ray diffraction which is utilized in Bragg Diffraction Ptychography (BDP). The BDP method was also shown to deliver detailed information on the strain field around single dislocations in silicon. With a focal spot as large as 1 μm , it was possible to resolve the strain with a resolution down to 50 nm. This value could be further improved by increasing the photon flux in the focal spot. BDP is a unique tool for the investigation of domain structures and domain wall configurations in complex ferroelectric and multiferroic thin film systems, which is hardly obtainable with any other method. Bragg diffraction ptychography is very relevant for the scientific case of the beamline. A constraint on its applicability could be the short focal length of the optics necessary to reach focal spots at the diffraction limit. However, improved methods of data evaluation with partially coherent beams could allow to overcome this condition and make it available for in situ measurements.

The following requirements were defined for the nanodiffraction beamline:

- It should implement X-ray diffraction based methods which make use of the high source brilliance and focus on in situ techniques, such as experiments under non-ambient conditions, time-resolved measurements and the investigation of growth processes and chemistry of low-dimensional and nanoscaled materials, as well as the study of functional materials in operando.
- Two separate experiment hutches should be available in an inline configuration, alternately sharing the beam from the undulator: one hutch for diffractometer based experiments and a second hutch for

accommodating rather large and complex instrumentation for sample growth and characterization including a UHV facility.

- The diffractometer must allow for heavy in situ sample environments for the investigation of growth, electrochemistry, chemical reactions, catalysis, etc.

- A set of dedicated sample cells should be developed for the beamline and be made available for user groups. The decision on the types of sample cells will be made later depending on user demand.

- The X-ray optics of the beamline should provide a high brilliance monochromatic beam in the energy range from 5 keV to 35 keV and a photon flux $\sim 10^{13}$ photons/sec at 10 keV.

- The beam spot at the sample position should vary from $\sim 0.3 \times 0.3$ mm² down to sub-micrometer dimensions.

1.3 Beamline layout.

Beamline P23 will be located in Hall East (PXE) of the PETRA III Extension (Fig. 1.3.1), sharing the sector with the Nano X-ray spectroscopy beamline P22.

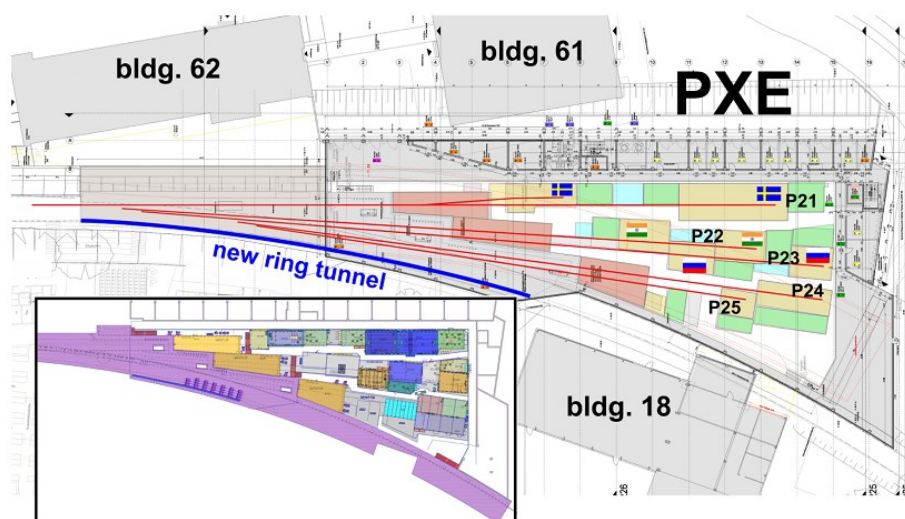


Figure 1.3.1. Schematic beamline arrangement and detailed floor plan (insert) of Hall East

Both undulators share the same straight section of the storage ring, beams are separated by a canting angle of 20 mrad. This proximity imposes some constraints on the geometrical configuration of the beamlines, both in the common X-ray optics hutch and the downstream experimental area. Beamline P23 will have a total length of 110 m and operate two endstations in two experimental hutches, EH1 (upstream) and EH2 (downstream). Both endstations share the same primary X-ray optics and will be operated alternately. The downstream hutch EH2 will be accessible during the operation of EH1, so that the instrumentation in EH2 can be used in off-line mode as well. The respective distances from the source are given in Table 1.4.1 and Figure 1.4.2. EH1 is 7.5 m long and 4 m wide, EH2 is 6.9 m long and 6.3 m wide. Control hutch one (CH1) is placed adjacent to EH1, while CH2 is placed above EH2 in order to gain additional floor space for the experiment. This option is not available for EH1 because of interference with the large crane servicing the optics hutches and frontend area.

2 Beamline optics

2.1 Necessary requirements to the beamline optics.

The following requirements for the beam parameters in nanoscale X-ray diffraction have been compiled:

- spot cleanliness. It is important to notice that high-resolution diffraction experiments are sensitive both to the spatial and angular distribution of the photons, in contrast to other techniques such as small angle X-ray scattering or chemical analysis microscopy.
- high stability against mechanical drifts and vibrations. To meet this requirement, demanding design efforts will be needed in case of in-situ sample environments and especially for heavy sample cells.
- focal distance. Long focal distances are very desirable not only to preserve a low beam divergence but also to leave sufficient space for larger sample environments. Obviously, longer distances lead to larger focal spot sizes and also additional challenges to handle stability issues.
- wavefront distortion for coherent beam experiments. The form of the incident wavefront is an important parameter in the data evaluation procedures used in coherent scattering methods. A complex wavefront profile that could arise due to optics imperfection can strongly impede the convergence of numerical evaluation procedures, while any instability in this parameter would in most case make the data evaluation completely impossible.
- maximal possible photon flux density in the focal spot.

Energy tunability and resolution at the beamline should be sufficient for XANES and resonant X-ray scattering measurements as well as for wavelength scans of Bragg reflections. The latter option can be, in many cases, a solution to the problem of sample displacements during angular scanning. The beamline optics must be designed to meet these requirements, but also to allow accommodation of further optical elements for future developments. The optical system should be reliably switchable between different configurations.

2.2 Beamline optics layout. Source properties

The focusing optics must provide focused beams at two endstations positioned in EH1 and EH2 at distances of ~ 88 m and ~ 108 m from the source. The targeted values of beam cross sections in different operation modes, as discussed above, vary from ~ 0.3 mm down to ~ 1 μm in an energy range from 4 keV to 35 keV. Smaller beams can be realized, but at the expense of reduced flux caused by limiting apertures.

It is planned to employ two main beam focusing schemes: mirror-based for energies below 15 keV and CRL-based for energies above 15 keV. There is a certain overlap of energy ranges optimal for both

approaches, which allows combined variants depending on the application. Moreover, at all energies the CRLs will be complemented with flat mirrors for harmonics suppression. The focusing elements close to the sample may also vary: for lower energies, KB systems will be preferably used. However, in some cases one might also utilize Fresnel zone plates, especially for ultra-compact and/or in-vacuum installations. For high energies, CRLs will be most effective and flexible for X-ray focusing. The distances between optical components and the source are summarized in Figure 17. Together with the source properties, they define the key parameters of possible optical configurations. There are also some specific technical boundary conditions that must be taken into account:

- it is not planned to use white beam mirrors in phase 1 of the beamline implementation. Therefore the mirror systems will be placed downstream of the monochromator.
- within the current generic frontend design it is not feasible to place larger optical components inside the ring tunnel. However, there is an option to insert water-cooled CRLs at ~43 m from the source.
- in the optics hutch, the P23 beam path runs close to the concrete shielding wall. For practical reasons, the closest position of the double-crystal monochromator (DCM) to the source is at 55 m.

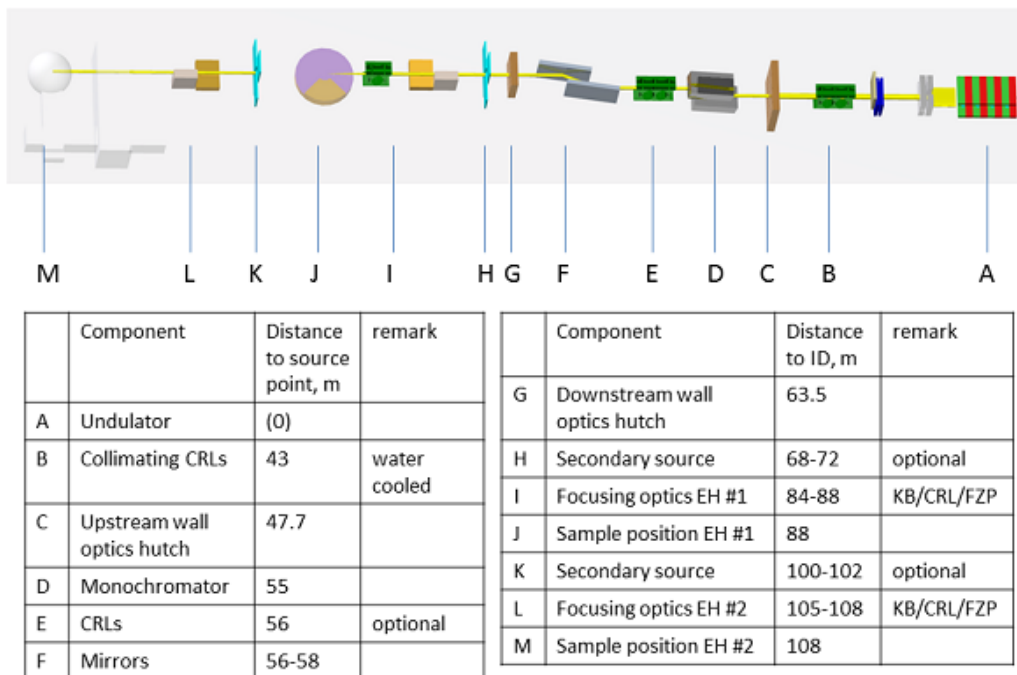


Figure 2.2.1. Distances to the main components of the X-ray optics

The initial beam after undulator has sizes $FWHM_{hor} = 0.332 \text{ mm}$, $FWHM_{ver} = 0.012 \text{ mm}$. First focusing optics is installed at 60 m from undulator. Since beam is divergent (and divergence depend on energy of photons) its size shown at fig. 2.2.2.

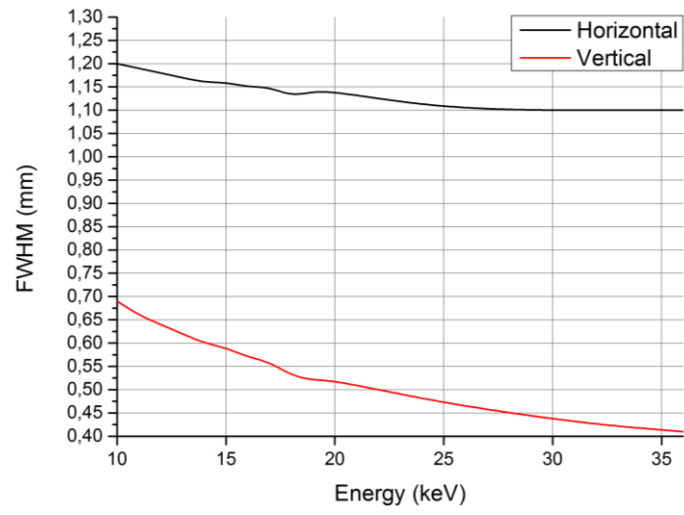


Figure 2.2.2

3 Focusing with lenses

3.1 Basic facts: geometrical optics

The lens-maker formula for a lens made from material with a refractive index n with radii of curvature of surfaces R_1, R_2 and distance d between them reads as:

$$\frac{1}{f} = (n - 1) \left(\frac{1}{R_1} - \frac{1}{R_2} + \frac{(n-1)d}{nR_1R_2} \right) \quad (3.1.1)$$

For a convex ($R_1 > 0, R_2 < 0$) thin lens ($d \ll |R_i|$) with equal radii of curvature R on both sides eq. 3.1.1 transforms to:

$$f = \frac{R}{2(n-1)} \quad (3.1.2)$$

A refractive index:

$$n = 1 - \delta + i\beta, \delta \sim 10^{-7} \div 10^{-5} > 0$$

$$\beta = \frac{\lambda\mu}{4\pi} \quad (3.1.3)$$

where μ (mm^{-1}) – linear absorption coefficient, λ – wavelength of photons. Since the mass absorption coefficient decreases with atomic number Z like Z^3 , the lens material is chosen to minimize absorption – e.g. aluminum or (even better) beryllium (fig. 3.1.1, right). On beamline P23 beryllium lenses will be used.

The real part of n for x-rays in any material is below 1 (for beryllium – fig. 3.1.1, left), it means that for converging x-ray lens R should be below zero, so the lens is concave (fig. 3.1.2) with focus:

$$f = \frac{R}{2\delta} \quad (3.1.4)$$

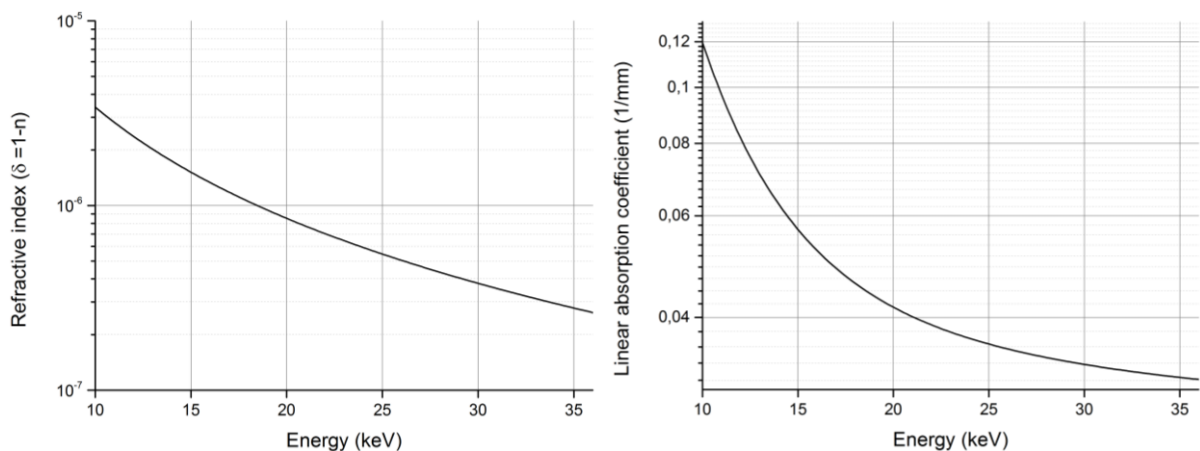


Figure 3.1.1. Refractive index and absorption coefficient vs x-rays energy for Be (from XOP)

In parabolic lens its surfaces are paraboloids of rotation given by:

$$z = \frac{r^2}{2R} \quad (3.1.5)$$

here z lies on the optical axis, r is perpendicular to it. The single lenses are about $l = 1 \text{ mm}$ thick and have distance between parabolic surfaces $d \approx 0.03 \text{ mm}$ (fig. 3.1.2). So aperture radius R_0 depends on the radius of curvature of parabola R as:

$$R_0 = \sqrt{(l-d)R}$$

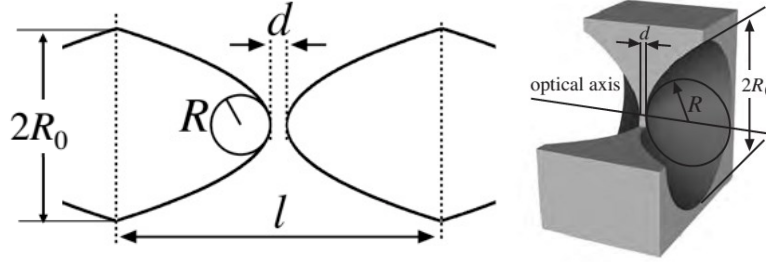


Figure 3.1.2. Parabolic lens

For a beryllium lens with a radius 1.5 mm at 15 keV ($\delta = 1.5 \cdot 10^{-6}$) focus distance will be $f = 1.5 \cdot 10^{-3} / 2 \cdot 1.5 \cdot 10^{-6} = 500 \text{ m}$. Therefore, to reach smaller focuses it's necessary to make a CRL. CRL with N individual lenses will have a focus:

$$f_N = \frac{R}{2N\delta} (1 + O(\delta)) \approx \frac{R}{2N\delta} \quad (3.1.6)$$

where the correction term (spherical aberration) is typically below 10^{-4} . Due to the large depth of field of refractive X-ray lenses and due to the large distances from source to CRL, from sample to CRL and large focus distance, the correction can be neglected for all practical purposes and a parabolic CRL can be considered as free of spherical aberration [1].

A distance a between object and thin lens and distance b between lens and image are connected with focus f like:

$$\frac{1}{f} = \frac{1}{a} + \frac{1}{b} \quad (3.1.7)$$

For a more common case of thick lens: a is distance from object to first principal plane and b – from second principal plane to image. Calculation of parameters for system made of only two thick lenses becomes quite difficult [2]. Another issue – equation (3.1.6) works only for one lens radius and number. If some different lens types appears in one transfocator it requires to consider them as some thick lenses. So, number of such thick lenses for system with two transfocators could reach 4-6 pieces. Therefore, using of “familiar” geometrical optics becomes very inconvenient. Another way to calculate parameters of CRL is described in the part 3.2

3.2 Coherent X-ray focusing. Ray transfer matrix analysis

Ray transfer matrix analysis is a type of ray tracing technique used in the design of laser optical systems. This technique uses the paraxial approximation of ray optics, which means that all rays are assumed to be at a small angle and a small distance relative to the optical axis of the system. It involves the construction of a ray transfer matrix (M) which describes the optical system; tracing of a light path through the system can then be performed by multiplying this matrix with a vector representing the light ray:

$$\begin{pmatrix} x_2 \\ \alpha_2 \end{pmatrix} = M \begin{pmatrix} x_1 \\ \alpha_1 \end{pmatrix}, M = \begin{pmatrix} A & B \\ C & D \end{pmatrix} \quad (3.2.1)$$

where x_1 and α_1 , x_2 and α_2 – coordinate and angle of the beam on the entrance and on the exit of optical system respectively (Fig. 3.2.1).

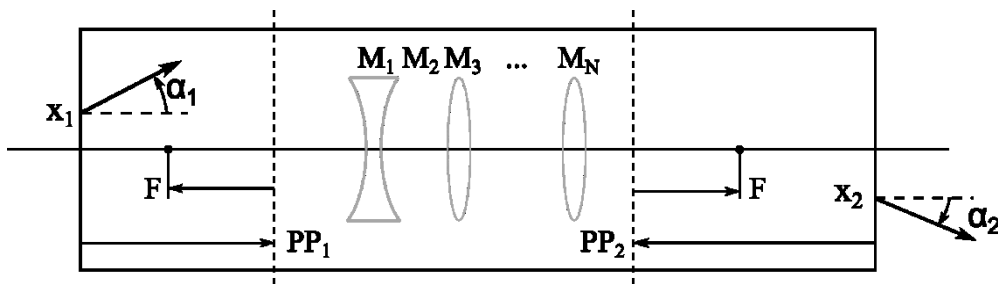


Figure 3.2.1. Schematic view of optical system

For a thin lens with focal length f matrix looks like:

$$M_L = \begin{pmatrix} 1 & 0 \\ -1/f & 0 \end{pmatrix} \quad (3.2.2)$$

For propagation on the distance d through a free space with refraction index n matrix is:

$$M_S = \begin{pmatrix} 1 & d/n \\ 0 & 1 \end{pmatrix} \quad (3.2.3)$$

To make a matrix of optical system it's necessary to multiply all matrices of single elements in reverse order. It means that if there are elements (from left to the right) with matrices M_1, M_2, \dots, M_N the matrix of optical system will be (see Figure 3.2.1):

$$M = M_N \cdot \dots \cdot M_2 \cdot M_1 \quad (3.2.4)$$

Matrix approach allows to determine location of cardinal points of optical system through A, B, C, D coefficients. Some of them are:

- Principal point 1 (measured from the entrance of system):

$$PP_1 = \frac{D-1}{C} \quad (3.2.5)$$

- Principal point 2 (measured from the exit of system):

$$PP_2 = \frac{1-A}{C} \quad (3.2.6)$$

- Focal points (measured from corresponding principal points):

$$F = -\frac{1}{C} \quad (3.2.7)$$

Another useful feature – matrix optics allows to investigate a propagation of Gaussian beams. It's assumed that beam is coherent. Gaussian beam is characterized by complex beam parameter q :

$$\frac{1}{q} = \frac{1}{R} - \frac{j}{\pi w^2} \quad (3.2.8)$$

here λ – wavelength of radiation, R – radius of curvature of wavefront:

$$R(z) = z \left(1 + \left(\frac{z_R}{z} \right)^2 \right), z_R = \frac{\pi w_0^2}{\lambda} \quad (3.2.9)$$

w – width of the beam ($FWHM = w \cdot \sqrt{2 \cdot \ln(2)}$):

$$w(z) = w_0 \sqrt{1 + \left(\frac{z}{z_R} \right)^2} \quad (3.2.10)$$

where z_R – Rayleigh range, w_0 – beam waist (minimal value of beam width).

When beam passes an optical system beam parameter changes by the “ABCD rule”:

$$\frac{1}{q_2} = \frac{C+D/q_1}{A+B/q_1} \quad (3.2.11)$$

Using this rule one can calculate new beam size and new radius of curvature of wavefront:

$$w_2 = \sqrt{-\frac{\lambda}{\pi \operatorname{Im}(1/q_2)}}, R_2 = \frac{1}{\operatorname{Re}(1/q_2)} \quad (3.2.12)$$

For the beam from undulator at beamline P23 it's known that it has size $w_u = 0.282 \text{ mm}$ (horizontal) – on the exit of undulator and w_{60} – after 60 m of propagation (depends on energy), but radii of curvature and beam waist w_0 are unknown. They could be calculated from eq. (3.2.10):

$$\begin{cases} w_u = w_0 \sqrt{1 + \left(\frac{z_0 \lambda}{\pi w_0^2} \right)^2} \\ w_{60} = w_0 \sqrt{1 + \left(\frac{(z_0 + \Delta z) \lambda}{\pi w_0^2} \right)^2} \end{cases} \quad (3.2.13)$$

here z_0 – distance from point when $w = w_0$ to exit of undulator, $\Delta z = 60000 \text{ mm}$ – distance from source to first transfocator. So, from (3.2.13):

$$\begin{aligned}
w_0 &= \sqrt{\frac{c^2 w_u^2 - 2ab + \sqrt{d}}{2(a^2 + c^2)}} \\
a &= \pi^2 (w_u^2 - w_{60}^2) \\
b &= \Delta z^2 \lambda^2 \\
c &= 2\Delta z \lambda \pi \\
d &= (2ab - c^2 w_u^2) - 4(a^2 + c^2)b^2
\end{aligned}
\tag{3.2.14}$$

4 Software implementation

Software is written in Python programming language with Python(x,y) development kit – it is a free scientific and engineering development software for numerical computations, data analysis and data visualization based on Python v.2.7.

Software for calculation parameters of CRL optic system has 3 modules:

- 1) Main module (“TS_matrix_optics_XX”) is responsible for:
 - Choosing and optimizing CRL transfocators in conformity with geometry of the setup and x-ray source properties.
 - Calculation ray transfer matrices for optical systems.
 - Calculation of beam size at any point of optical system.
 - Managing other modules and general calculation flow.

This module is described in details in 4.1.

- 2) Module for calculation of photon flux transmitted through transfocators (“TS_transmission_gauss_module_XX”). The description is in part 4.2.
- 3) Service module (“TS_read_data”) which is used for reading miscellaneous data (initial beam sizes, optical constants, etc.) from hard disk. It has 3 functions:
 - `size_calc` – reads size of beam (FWHM) on 60 m from undulator for chosen energy of photons.
 - `delta_calc` – reads refraction index for chosen x-ray energy.
 - `mu_calc` – reads linear absorption coefficient for chosen energy (Energy) of photons.

Note: In modules functions/classes with names started from “_” are used only as an auxiliary ones for other modules/classes. Only “user-available” functions will be described below.

4.1 General calculation flow, optics optimization and geometry

The current version of software allows to calculate parameters of two transfocators (and their combinations) from given lens setup and, vice versa, to select best combination of lenses in transfocators to achieve desirable imaging conditions.

In software transfocators are represented as list objects in format:

$$[[N1, N2, \dots], [R1, R2, \dots], [d1, d2, \dots], 1]$$

here N_i – number of lenses one type, R_i – radius of curvature of parabola, d_i – distance between peaks of parabolic surfaces in lens, l – thickness of one lens (see part 3.1).

Global input parameters are:

– `energy_min`, `energy_max`, `energy_step` – range of energy for calculation: [`energy_min`, `energy_max`] with step `energy_step`.

- `dist_Src_TS1`, `dist_TS1_TS2`, `dist_TS2_Sample` – distances from undulator to first transfocator, between transfocators, from second transfocator to sample respectively.
- `dist_TS1_image1` (`dist_TS2_image2`) – desirable distance from first (second) transfocator to image created by it.
- `Source_hor_0` (`Source_ver_0`) – beam size (FWHM) on the exit of the undulator.
- `R_set1` (`R_set2`) – list of radii of lenses that are allowed to use in first (second) transfocator.
- `lens_groups11` (`lens_groups21`) – groups of lenses of 1st radius that are allowed to use in 1st (2nd) transfocator.
- `lens_groups12` (`lens_groups22`) – groups of lenses of 2nd radius that are allowed to use in 1st (2nd) transfocator.

Choosing the transfocator

`build_TS_from_dist` – Makes a list of transfocators from specified group of lenses with specified radii which create an image of object on appropriate distance from transfocator.

Matrix optics

`All_elements` (class) – the object of this class is a list of all elements in optical system. This list contains an index number of the element, information about type of element (free space or lens) and parameter of every element (length of space or focus of lens), it looks like:

n	type	parameter
0	'space'	60000
1	'lens'	495000
2	'space'	1
3	'lens'	495000
...

`system_matrix` – makes a matrix of optical system from the list of elements ('`All_elements`' class object). It uses matrix formalism from part 3.2 (eq. 3.2.1 – 3.2.4).

`cardinal_points` – calculates distances to cardinal points of the optical system – see eq. 3.2.5 - 3.2.7

Beam size calculation

`size_calc_geometry` – calculates size of beam on the out of optical system using conventional geometrical optics laws:

$$\frac{1}{f} = \frac{1}{a} + \frac{1}{b}, \frac{b}{a} = \frac{h_{out}}{h_{in}} \quad (4.1.1)$$

here a is distance from object to first principal plane, b – from second principal plane to image, h_{in} – size of object and h_{out} – size of image in the image plane. To know size of beam not only in image plane, approximate equation is used:

$$h_{out}^* = h_{out} + |x_{out}| \quad (4.1.2)$$

where x_{out} – coordinate of beam that entered the system at optical axis with angle $\theta/2$ (θ – beam divergency):

$$\begin{pmatrix} x_{out} \\ \alpha_{out} \end{pmatrix} = \begin{pmatrix} A & B \\ C & D \end{pmatrix} \begin{pmatrix} 0 \\ \theta/2 \end{pmatrix} \quad (4.1.3)$$

size_calc_wave_parameter – calculates beam size from transformation of complex beam parameter– see eq. 3.2.8 – 3.2.13.

4.2 Transmission and beam loss factor

Absorption of monochromatic beam in matter is described with Beer–Lambert law:

$$I = I_0 \exp(-\mu x) \quad (4.2.1)$$

where μ is a linear absorption coefficient, x – thickness of material, I_0 and I – initial intensity of x-rays and intensity after propagation through material.

For a CRL with N parabolic lenses with radius of aperture R_0 , radius of curvature of parabolas R and distance d between parabolas (fig. 3.1.2) beam loss factor is [3]:

$$T = \frac{I}{I_0} = \exp(-\mu N d) \frac{1}{a_p} (1 - \exp(-a_p)) \quad (4.2.2)$$

$$a_p = \frac{\mu N R_0^2}{R}$$

Unfortunately, this equation works only for beams with uniform distribution of intensity. For beam with Gaussian distribution (with standard deviations σ_x , σ_y in horizontal and vertical directions) of intensity:

$$I_0 = A \exp\left(-\frac{x^2}{2\sigma_x^2}\right) \exp\left(-\frac{y^2}{2\sigma_y^2}\right) \quad (4.2.3)$$

beam loss factor is calculated analytically in quite complex way [1]. But it's easy to calculate beam loss factor numerically: just use eq. 4.2.1 in every point of every lens and then divide sum of intensity after the CRL by sum of intensity before CRL.

There is only one user-available function in TS_transmission_gauss_module: calculate – it calculates the transmission numerically as described above. One important thing – it's assumed that paraxial approximation for optical system is working (== size of beam is changed negligible during propagation through CRL).

4.3 Output

As a result software creates text file for every transfocator with table of lens combinations for specified range of energies with calculated focus, beam loss factor and size of beam. Example of such list – see figure 4.3.1. Legend for a table:

- E(eV) – energy of photons
- R – radii of curvature of lens parabola
- N – corresponding number of lenses
- F_pos – coordinate of focus (from undulator)
- Im_pos – coordinate of image (from undulator)
- T – transmitted amount of light
- HorSize (VerSize) – horizontal (vertical) FWHM of beam (at the entrance of 2nd transfocator or on sample)

```

Transfocator system #1
Image pos = 27000.0 mm
Lens radii: [0.5, 0.3]
Groups of lenses: [2, 3, 5, 13] [2, 3, 5, 13]
Src - TS1 = 60000.0 mm
TS1 - TS2 = 27000.0 mm
TS2 - Sample = 0.0 mm

```

E(eV)	R	N	F_pos	Im_pos	T	HorSize	VerSize
20000	[0.5, 0.3]	[16, 0]	78327.1104118	86393.6967111	0.66583832836	0.164167270885	0.0166585945132
20000	[0.5, 0.3]	[7, 5]	79126.21985	88080.125612	0.589820809499	0.186781603396	0.0253547639009
20000	[0.5, 0.3]	[2, 8]	79126.4074976	88080.161481	0.591296581479	0.186725576531	0.0253191776248
20000	[0.5, 0.3]	[3, 8]	77955.0369129	85626.2964984	0.585649136913	0.184804913778	0.0321566309268
20000	[0.5, 0.3]	[8, 5]	77954.796554	85626.2632159	0.584187459959	0.184743192144	0.0321175844269
21000	[0.5, 0.3]	[13, 3]	77962.3589893	85643.0659687	0.583226183042	0.1837955355	0.0311869185716
21000	[0.5, 0.3]	[18, 0]	77960.8647167	85641.7576054	0.661275514987	0.183775099009	0.0311732476392
21000	[0.5, 0.3]	[0, 10]	79400.8342121	88675.8457011	0.590842073791	0.205741488731	0.0350109267448
21000	[0.5, 0.3]	[5, 7]	79400.7762022	88675.9144072	0.592278335706	0.205771453004	0.0350294572241
21000	[0.5, 0.3]	[5, 8]	77636.48311	84982.919315	0.583794155601	0.202492719255	0.0449616394025
22000	[0.5, 0.3]	[16, 2]	78353.2592554	86448.1313034	0.583816454647	0.162402911172	0.0151579153073
22000	[0.5, 0.3]	[7, 7]	79010.3659665	87831.9252677	0.589507707174	0.178087607259	0.0203804213476
22000	[0.5, 0.3]	[2, 10]	79010.4925855	87831.972117	0.590882157559	0.178033217099	0.0203460888922
22000	[0.5, 0.3]	[3, 10]	78043.4867834	85807.6623303	0.585749886818	0.179082110515	0.0274788812665
22000	[0.5, 0.3]	[8, 7]	78043.3209907	85807.6414083	0.584387374604	0.179020969252	0.0274415164851
23000	[0.5, 0.3]	[16, 3]	78468.0039006	86687.1856414	0.584136152367	0.156366833211	0.0106179298039
23000	[0.5, 0.3]	[21, 0]	78466.4434491	86685.7973296	0.655930117618	0.1563502264	0.0106069760194
23000	[0.5, 0.3]	[8, 8]	78180.3840734	86089.2790697	0.584711254689	0.171341796678	0.021627785132
23000	[0.5, 0.3]	[13, 5]	78179.8915374	86089.1154379	0.583389856289	0.171288219822	0.0215939812369
23000	[0.5, 0.3]	[18, 2]	78178.8276586	86088.3605393	0.582071444138	0.171252810613	0.0215709751373
24000	[0.5, 0.3]	[18, 3]	78360.010734	86463.1803532	0.583736067705	0.16164587914	0.0144319169115
24000	[0.5, 0.3]	[23, 0]	78358.4149462	86461.743603	0.652085412577	0.161630563009	0.0144219213168
24000	[0.5, 0.3]	[10, 8]	78098.8022044	85922.3290423	0.584312192202	0.175284261971	0.0243320298895
24000	[0.5, 0.3]	[15, 5]	78098.2214614	85922.0908141	0.58302425475	0.17523325399	0.0242999947579
24000	[0.5, 0.3]	[20, 2]	78097.0896542	85921.2528519	0.581739156163	0.175200305263	0.0242787790117
25000	[0.5, 0.3]	[3, 13]	78576.9389971	86914.1551808	0.585558293152	0.150984706121	0.00659550531577
25000	[0.5, 0.3]	[8, 10]	78576.8336002	86914.1111687	0.584295933777	0.150926741949	0.00656199652524
25000	[0.5, 0.3]	[13, 7]	78576.4651732	86914.0422357	0.583036295824	0.150872565952	0.00652900189264
25000	[0.5, 0.3]	[21, 2]	78829.4686021	87450.4820236	0.582461008566	0.165266579811	0.0134158401398
25000	[0.5, 0.3]	[16, 5]	78830.6309085	87451.3415787	0.583719403623	0.165232137263	0.0133967508435

Figure 4.3.1 – Example of list of transfocators

5 Application examples

The typical distances between optical components in P23 could be: undulator - transfocator 1 – 60 m, transfocator 1 - transfocator 2 – 26 m, transfocator 2 - sample – 1 m. This values will be used for examples in this chapter.

5.1 Single transfocator

The simplest optical system is one transfocator that focuses the beam onto the sample, so distance from transfocator to image will be

$$(\text{dist. transf.1 transf.2}) + (\text{dist. transf.2 - sample}) = 27 \text{ m}$$

To calculate size of beam geometrical optics approach was used. From figures 5.1.1 – 5.1.2 it's seen that it makes no sense to use lenses with 1.5 and 1.0 radii especially on higher energies because their number becomes too large and transmission decreases.

```
Transfocator system #1
Image pos = 27000.0 mm
Lens radii: [0.5, 0.3]
Groups of lenses: [2, 3, 5, 13] [2, 3, 5, 13]
Src - TS1 = 60000.0 mm
TS1 - TS2 = 27000.0 mm
TS2 - Sample = 0.0 mm
```

E(eV)	R	N	F_pos	Im_pos	T	HorSize	VerSize
15000	[0.5, 0.3]	[0, 5]	79794.0510492	89540.7154784	0.581056935365	0.234814398518	0.0557173831252
15000	[0.5, 0.3]	[5, 2]	79793.8190311	89540.8380946	0.582821750167	0.234847502334	0.0557385665398
15000	[0.5, 0.3]	[5, 3]	76494.3536086	82750.0111471	0.570223387587	0.280307602761	0.112343110571
15000	[0.5, 0.3]	[10, 0]	76493.1924302	82749.0838407	0.665886672027	0.280268084322	0.112314120677
15000	[0.5, 0.3]	[8, 0]	80617.8656365	91415.6736485	0.690805636347	0.290401618071	0.0876495318181
16000	[0.5, 0.3]	[10, 0]	78766.7540376	87312.2851538	0.682617822344	0.160763135046	0.0120263317082
16000	[0.5, 0.3]	[5, 3]	78767.9152079	87313.1711315	0.585438037199	0.16072777053	0.0120035891151
16000	[0.5, 0.3]	[2, 5]	78162.5315495	86049.4746169	0.584221581481	0.173805636181	0.0254416509078
16000	[0.5, 0.3]	[7, 2]	78162.1183966	86049.332554	0.582393335447	0.173748346116	0.025401717049
16000	[0.5, 0.3]	[3, 5]	76559.5987576	82874.3668205	0.57698559775	0.273854686711	0.10503877274
17000	[0.5, 0.3]	[8, 2]	78694.4840967	87158.8850678	0.583854259838	0.155345218888	0.00881942179217
17000	[0.5, 0.3]	[3, 5]	78694.9832837	87159.0717213	0.585561235848	0.155288905269	0.00878281091667
17000	[0.5, 0.3]	[0, 7]	78160.7484637	86046.020424	0.580355802162	0.173867654715	0.0251326398703
17000	[0.5, 0.3]	[7, 3]	77655.853398	85020.7177001	0.579940000768	0.202867544418	0.0481542311182
17000	[0.5, 0.3]	[7, 2]	80504.1530402	91152.2651541	0.590665871614	0.281619127236	0.0794110860313
33000	[0.5, 0.3]	[8, 21]	78565.8042686	86895.6171018	0.546808570448	0.151035343719	0.00654229876463
33000	[0.5, 0.3]	[13, 18]	78565.6830059	86895.5950786	0.545757565342	0.150977722451	0.00651217456227
33000	[0.5, 0.3]	[18, 15]	78565.4210641	86895.5801011	0.544708580342	0.150921775436	0.00648199739141
33000	[0.5, 0.3]	[21, 13]	78710.3390155	87201.0477228	0.545170283377	0.157151930518	0.00896196334184
33000	[0.5, 0.3]	[16, 16]	78710.71717	87201.1144288	0.546220157511	0.157095839059	0.0089328619732
34000	[0.5, 0.3]	[7, 23]	78693.4443704	87164.8090326	0.541855131813	0.155824421728	0.00832660818566
34000	[0.5, 0.3]	[16, 18]	78422.0315304	86596.2751858	0.537887627119	0.157902862058	0.0109714324046
34000	[0.5, 0.3]	[21, 15]	78421.7061795	86596.2340088	0.536863642103	0.157847508378	0.0109415715141
34000	[0.5, 0.3]	[20, 15]	78831.5406276	87458.1801557	0.540236698909	0.165731539552	0.0127597228425
34000	[0.5, 0.3]	[15, 18]	78831.8450209	87458.2077933	0.541267117514	0.165675424734	0.0127306136294
35000	[0.5, 0.3]	[10, 23]	78579.185634	86925.1233267	0.534142869309	0.150244464013	0.00602593717705
35000	[0.5, 0.3]	[15, 20]	78579.0502486	86925.1090891	0.533134876619	0.1501869447	0.00599628595671
35000	[0.5, 0.3]	[23, 15]	78707.6917798	87196.9230941	0.532548765536	0.157130358834	0.00889535514131
35000	[0.5, 0.3]	[18, 18]	78708.0583268	87196.9824318	0.533555650072	0.157074113284	0.00886667448075
35000	[0.5, 0.3]	[13, 21]	78708.2685509	87196.9862527	0.534564438314	0.157017608587	0.00883719191794

Figure 5.1.1. List of transfocators made from 0.5 and 0.3 mm lenses

Transfocator system #1
 Image pos = 27000.0 mm
 Lens radii: [1.5, 1.0]
 Groups of lenses: [2, 3, 5, 13, 21, 34] [2, 3, 5, 13, 21, 34]
 Src - TS1 = 60000.0 mm
 TS1 - TS2 = 27000.0 mm
 TS2 - Sample = 0.0 mm

E(ev)	R	N	F_pos	Im_pos	T	HorSize	VerSize
15000	[1.5, 1.0]	[16, 7]	78668.7201148	87109.655757	0.73427933349	0.154052082492	0.00822937310939
15000	[1.5, 1.0]	[7, 13]	78669.3130171	87109.809562	0.738042648778	0.15396311483	0.00816866237527
15000	[1.5, 1.0]	[3, 16]	78323.4227573	86386.8077739	0.736576660212	0.164704969893	0.0183136848644
15000	[1.5, 1.0]	[0, 18]	78323.4265308	86386.7452243	0.737297534287	0.164706244613	0.018315096674
15000	[1.5, 1.0]	[15, 8]	78322.9136887	86386.6676583	0.731573134015	0.164583968072	0.0182291427134
16000	[1.5, 1.0]	[18, 8]	78762.7101213	87309.4161857	0.732921094223	0.161155046814	0.012294592285
16000	[1.5, 1.0]	[15, 10]	78763.0132663	87309.5365144	0.734070583796	0.161127540861	0.012276632843
16000	[1.5, 1.0]	[0, 20]	78763.4286824	87309.5887328	0.73953501143	0.161009593226	0.0121959815234
16000	[1.5, 1.0]	[3, 18]	78763.4256257	87309.6485112	0.738686598605	0.161012068772	0.0121971965582
16000	[1.5, 1.0]	[8, 15]	78455.5587953	86662.7063335	0.73394867603	0.157230965244	0.011930818685
17000	[1.5, 1.0]	[34, 0]	78685.9603412	87152.3829424	0.729381582826	0.15587620208	0.00917250980201
17000	[1.5, 1.0]	[31, 2]	78686.8745298	87153.2598168	0.721092529602	0.155872179267	0.00917002197387
17000	[1.5, 1.0]	[10, 16]	78689.6409974	87154.9802148	0.728498271499	0.155706550166	0.00906341980829
17000	[1.5, 1.0]	[7, 18]	78689.703955	87154.9891357	0.729562425329	0.155677226086	0.00904342975158
17000	[1.5, 1.0]	[3, 21]	78418.654973	86586.894143	0.72842689327	0.159145744986	0.0133575197024
33000	[1.5, 1.0]	[73, 37]	78615.5329266	87031.405455	0.564571584965	0.153683070661	0.00753470068716
33000	[1.5, 1.0]	[70, 39]	78615.8429531	87031.532681	0.565114941812	0.153657058607	0.00752146998077
33000	[1.5, 1.0]	[58, 47]	78616.8393645	87031.8343864	0.567293603631	0.153547834068	0.00746542677195
33000	[1.5, 1.0]	[55, 49]	78617.032992	87031.8694913	0.567839580213	0.153519621689	0.00745081101259
33000	[1.5, 1.0]	[34, 63]	78617.8891953	87031.9207665	0.571676157536	0.153320677523	0.00734565109422
34000	[1.5, 1.0]	[78, 39]	78600.8554795	87003.2611942	0.552551961475	0.152938693121	0.00719474611375
34000	[1.5, 1.0]	[75, 41]	78601.1700205	87003.3927573	0.553078664482	0.152912765609	0.00718168550609
34000	[1.5, 1.0]	[63, 49]	78602.1960909	87003.7182519	0.555190501932	0.152803986225	0.00712644477487
34000	[1.5, 1.0]	[54, 55]	78602.7489854	87003.8085086	0.556779670138	0.152719005481	0.00708272839685
34000	[1.5, 1.0]	[42, 63]	78603.2469074	87003.8280832	0.558905639253	0.152604703489	0.00702297422147
35000	[1.5, 1.0]	[71, 49]	78619.2041836	87042.6478834	0.543128761758	0.154355113617	0.00781266066218
35000	[1.5, 1.0]	[62, 55]	78619.8414789	87042.7909453	0.544669821642	0.154271325801	0.00777019775324
35000	[1.5, 1.0]	[50, 63]	78620.4454655	87042.8453204	0.546731372065	0.154157268039	0.00771158663768
35000	[1.5, 1.0]	[47, 65]	78620.5583306	87042.8466705	0.547247977718	0.154128744583	0.00769675914998
35000	[1.5, 1.0]	[28, 78]	78556.5644596	86907.5868294	0.54969003839	0.149377570972	0.00557398218698

Figure 5.1.2. List of transfocator made from 1.5 and 1.0 mm lenses

5.2 Two transfocators (parallel beam)

Another important case – to make a parallel beam (telescope). It means that image plane of 1st transfocator should be matched with a focal plane of the second transfocator. Results for such transfocator system is in fig.5.2.1.

Transfocator system #1
 Image pos = 20000.0 mm
 Lens radii: [0.5, 0.3]
 Groups of lenses: [2, 3, 5, 13] [2, 3, 5, 13]
 Src - TS1 = 60000.0 mm
 TS1 - TS2 = 26000.0 mm
 TS2 - Sample = 1000.0 mm

E(eV)	R	N	F_pos	Im_pos	T	HorSize	VerSize
15000	[0.5, 0.3]	[3, 5]	74553.5149918	79215.9158674	0.561197413928	0.398330392381	0.207673974478
15000	[0.5, 0.3]	[8, 2]	74553.01579	79215.6614726	0.559288073753	0.398251450013	0.207617451627
15000	[0.5, 0.3]	[0, 7]	74137.6078363	78497.4422172	0.556571356837	0.437853490321	0.237895389863
15000	[0.5, 0.3]	[7, 2]	75961.8974897	81749.8453365	0.566978672804	0.281841073462	0.117075171878
15000	[0.5, 0.3]	[2, 5]	75962.3106484	81750.0147035	0.568914267731	0.281911311683	0.117125273621
16000	[0.5, 0.3]	[8, 3]	74435.6368314	79011.7700622	0.564029899266	0.405416906158	0.208587530774
16000	[0.5, 0.3]	[13, 0]	74434.3106299	79010.6176708	0.649996324785	0.405376943718	0.208559050684
16000	[0.5, 0.3]	[7, 3]	75639.1013391	81155.1659746	0.571038688412	0.304037204396	0.131771202023
16000	[0.5, 0.3]	[5, 5]	74074.9248748	78390.8071478	0.562896199209	0.439779899861	0.234249054919
16000	[0.5, 0.3]	[0, 8]	74075.0155168	78390.7554327	0.560884864531	0.439829693362	0.234283862091
17000	[0.5, 0.3]	[2, 7]	75502.4050975	80905.7156699	0.571167151657	0.314686156302	0.137494288958
17000	[0.5, 0.3]	[3, 7]	74445.0596545	79027.9130671	0.564691073881	0.404602317894	0.204315792901
17000	[0.5, 0.3]	[10, 3]	74123.3646631	78474.4753654	0.560370534793	0.434863148506	0.226526262697
17000	[0.5, 0.3]	[15, 0]	74121.9596096	78473.2247601	0.642277148509	0.434826065009	0.226500319988
17000	[0.5, 0.3]	[10, 2]	75889.3485151	81616.4142262	0.570566826819	0.285070509731	0.115159181225

Figure 5.2.1. 1st transfocators for telescope

Transfocator system #1 + #2
 Image pos = 100000000.0 mm
 Lens radii: [0.1]
 Groups of lenses: [2, 3, 5, 8, 13, 21, 34] [2, 3, 5, 8, 13, 21, 34]
 Src - TS1 = 60000.0 mm
 TS1 - TS2 = 26000.0 mm
 TS2 - Sample = 1000.0 mm

E(eV)	R	N	F(TS2)	F_pos	Im_pos	T	HorSize	VerSize
15000	[0.1, 0]	[8, 0]	4125.32343925	93008.4637111	229437.484019	0.915051976689	1.22495807009	0.258989698085
15000	[0.1, 0]	[10, 0]	3300.85909798	90923.0467135	100803.199951	0.897519879923	0.570087660525	0.120453562916
15000	[0.1, 0]	[11, 0]	3001.09942797	90286.2456568	96223.573306	0.888987336603	0.435448998513	0.112376055144
15000	[0.1, 0]	[13, 0]	2540.00783825	89406.4894073	92318.9375083	0.872368905142	0.315088640281	0.101614349693
15000	[0.1, 0]	[15, 0]	2201.96321488	88827.6662307	90575.2740975	0.856320416921	0.255986669165	0.093081803397
16000	[0.1, 0]	[7, 0]	5363.88707637	96012.8097396	109165.44063	0.787170202267	0.636491233895	0.20864587672
16000	[0.1, 0]	[8, 0]	4693.7138009	93907.0953524	100329.62274	0.774983997823	0.495344598102	0.198413580664
16000	[0.1, 0]	[10, 0]	3755.57134531	91567.7089256	94131.7230085	0.751506888498	0.38604000988	0.184218301136
16000	[0.1, 0]	[11, 0]	3414.47416822	90850.9957479	92687.1097971	0.740197341337	0.356339652468	0.178031164296
16000	[0.1, 0]	[13, 0]	2889.78638826	89858.9854027	90935.7655691	0.718392128796	0.314119889248	0.166295814305
17000	[0.1, 0]	[7, 0]	6055.34490055	98367.553276	117165.460317	0.932018189271	0.746005897248	0.231085533149
17000	[0.1, 0]	[8, 0]	5298.7393846	95576.4796405	103963.424377	0.924105866877	0.558586227027	0.219371077174
17000	[0.1, 0]	[10, 0]	4239.59177747	92600.1344814	95727.8824228	0.908653962534	0.430960681153	0.20489346913
17000	[0.1, 0]	[11, 0]	3854.49271801	91713.259382	93915.1733825	0.901108619341	0.398521907657	0.198796829054
17000	[0.1, 0]	[13, 0]	3262.10971328	90504.3346591	91768.0348779	0.886365365509	0.35378350697	0.187348373037

Figure 5.2.2. 2nd transfocators for telescope

5.3 Two transfocators (“aperture matching”)

“Aperture matching” means that first transfocator pre-focuses beam to aperture of the second one. The second transfocator should have a quite short focus distance in this case. This approach allows to achieve smallest spot on the sample. After tests of transfocators made from lenses with radii 1.5, 1.0, 0.5, 0.3, 0.1 mm, was concluded that transfocator with best transmission coefficient for whole range of energies could be built from 0.5, 0.3 mm (1st tr.) and 0.1 mm (2nd tr.) lenses (fig. 5.3.1-5.3.2).

5.4 Selection of beam size calculation method

On figure 5.4.1 horizontal and vertical size of beam after the out of second transfocator (aperture matching case) are shown. Size was calculated by geometrical optics (4.1) and using wave parameter approach (3.2).

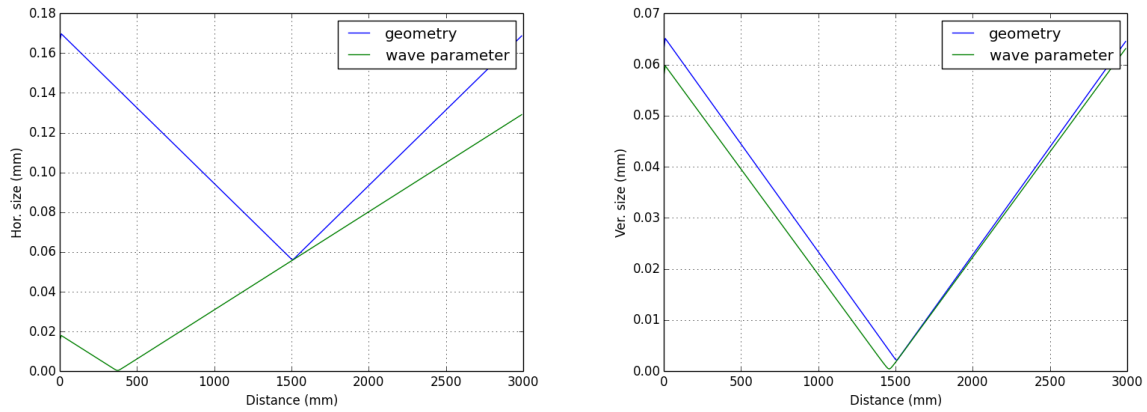


Figure 5.4.2. Beam size after 2nd transfocator

Such large difference could be explained by fact that wave parameter approach is valid only for coherent beams, while the radiation after undulator has both coherent and incoherent fractions (fig. 5.4.2).

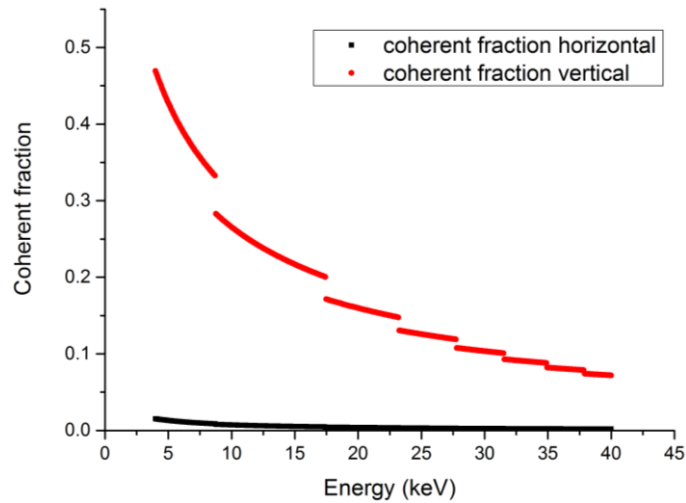


Figure 5.4.2. Coherent fraction of x-rays from undulator

Conclusion

A new software package was created, tested and used for beamline CRL optics design. Software is written in Python, has a modular structure. Typical scenarios of beamline CRL layout were tested: one transfocator, telescope, aperture matching. The modules developed in this work will become a part of beamline operation software at the Russian-German nanodiffraction beamline at PETRA.

Acknowledgement

I would like to thank Jana Raabe for her friendly support and cooperation during my stay at DESY.

References

- [1] B. Lengeler et al., Imaging by parabolic refractive lenses in the hard X-ray range, (2000)
- [2] Eugene Hecht, Optics, (2002)
- [3] B. Lengeler et al., Transmission and gain of singly and doubly focusing refractive x-ray lenses, (1998)